Lidar ratio of Asian haze and pollution episodes observed by using a Raman/elastic lidar

Zhenyi Chen (陈臻懿)[1*], Wenqing Liu (刘文清)[1], Yujun Zhang (张玉钧)[1], and Birgit Heese[2]

[1] *Key Laboratory of Environmental Optics and Technology, Anhui Insititute of Optics and Fine Mechanics, Hefei 230031, China;*

[2] *Institute of Tropospheric Research, Leipzig, Germany*

[*] *Corresponding author: zychen@aiofm.ac.cn*

Received August 8, 2011; accepted October 24, 2011; posted online April 25, 2012

A combined Raman/elastic backscatter lidar observations is carried out in the Pearl River Delta (PRD) China. The results show the largest lidar ratios of the order of 80 sr in the uplifting boundary layer in 2-3 km during the haze period. In the moderate pollution period, the lidar ratio has an average value of 58 sr. The Angstrom exponent exhibits high values around 1.82, indicating the presence of rather small particles. Different back air mass trajectories and the ambient atmospheric conditions are attributed to the distinct characteristics of aerosol optical properties in the haze and moderate pollution episodes. In the lower layer in the haze period, air masses are mostly advected from southeast coast China. In contrast, the air mass in the moderate pollution observing period passes through northwest China, indicating the combination of some pollution from the Tarim Basin in case of strong convection and the smoke from adjacent fire burning spot in PRD region.

OCIS codes: 010.0100, 210.4770, 180.1790.

doi: 10.3788/COL201210.S10101.

Atmospheric aerosols, which originate both from natural sources and from human intervention, considerably affect the Earth's radiation balance. It can also have great impact on the near-ground atmosphere and thus the human life. In the past 20 years, with increased population and quick development, the Pear River Delta (PRD) in southeast China faces high aerosol concentrations that lead to low visibility, 50% of days in 2006 had visibility <1 km in Shenzhen[1−3]. Raman lidar is a widely used method to measure the extinction coefficient and backscattering coefficient of aerosols simultaneously and independently of each other[4,5]. The advantage of this method is that no critical assumptions on atmospheric input parameters are needed for data analysis. And the extinction-to-backscatter ratio obtained from Raman lidar can be used to identify the aerosol types[6−9]. It is also possible to separate the impact of natural and anthropogenic on aerosols, or notify the aerosol sources combining this quantity with air masses transportation[10,11]. Furthermore, an unambiguous lidar ratio S is essential to properly retrieve backscatter coefficient profiles[12]. Although elastic lidar observations have been conducted at several sites in China in the past few years, direct measurements of S are still needed to be performed to get more optical characteristics, vertical distribution and sources of atmospheric aerosols over South China.

A combined Raman (355-387)/ elastic (532) backscatter lidar (see Fig. 1) was carried out in Zhongshan, PRD China, from Nov. 22 to Dec. 5, 2009 as a part of a joint Sino-Germany campaign performed by Anhui Institute of Optics and Fine Mechanics (AIOFM), China, Institute of Tropospheric Research (IFT), Leipzig and Institute of Remote Sensing Applications (IRSA), China. The aerosol optical parameters, such as backscatter coefficient, extinction coefficient, lidar ratio for 355 nm, and related aerosol optical properties are observed.

Our measurements were performed in Zhongshan (22.53N, 113.38E see Fig. 2), which is located in PRD and served as midway between Guangzhou and Macao. Zhongshan is chosen as a key geographical position, where different aerosols sources are, such as maritime aerosols from South China Sea, anthropogenic aerosols from the highly populated urban centers and industrial areas, as well as biomass burning aerosols coexist. In this letter, the data in two periods, from Nov. 27 to Nov. 30 (the haze period) and from Dec. 2 to Dec. 4 (moderate pollution period), are discussed. Figure 2(a) is the map of China colored by population density (km^{-2}). Figure 2(b) labels the observation site, Zhongshan and other major cities in PRD.

The pulsed Nd:YAG laser emits short pulses at 532 and 355 nm. The pulse repetition rate is typically 20 Hz. The pulse duration is of the order of 6-9 ns. The beam expansion factor is equal to 4 for 355 and 532. The receiving telescope of the lidar system is based on a Cassegrain

Fig. 1. Raman/Elastic lidar.

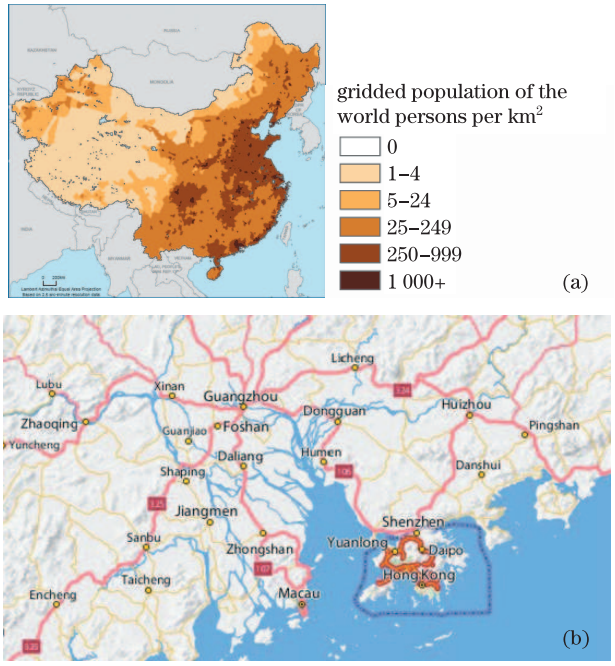

Fig. 2. (a) Map of China colored by population density (km^{-2}). Socioeconomic data and application center of the Columbia University; (b) observation sites and near cities in PRD, China. (http://travel.yahoo.com/p-map-482573-map_of_zhongshan).

design. The primary reflective mirror has a diameter of 400 mm and is coated with a durable high reflective coating suitable for the 350–1 100-nm spectral region. Analog detection of the photomultiplier current and single photon counting is combined in one acquisition system. The combination of a powerful A/D converter (12 Bit at 40 MHz) with a 250 MHz fast photon counting system increases the dynamic range of the backscattered signal substantially compared with conventional systems.

For the elastic-backscatter signal at 355 nm and its nitrogen inelastic-backscatter signal at 387 nm, vertically resolved particle backscatter coefficients, extinction coefficients, and extinction-to-backscatter (lidar ratio) S profiles can be retrieved based on the methodology described by Ansmann *et al.*[5] The measurement was performed day and night, only nighttime data (from 18:00 to 22:00 local time) were used in the analysis for Raman channel because of the large background radiation in the daytime. The range resolution is 15 m in the data processing for both of the elastic and the Raman signals. Profiles of lidar ratio and Angstrom exponent can also be confirmed from aerosol extinction and backscattering profiles. Relative humidity (RH) and potential temperature (PT) are presented from NOAA HYSPLIT.

The NOAA/ARL HYSPLIT mode was used to calculate the backward trajectories of air masses during our observation period[13]. The heights were fixed at 1, 1.5, and 2.5 km since most of the aerosol layers were detected below 3 km. The word fire atlas hotspot detection is also applied to notify the smoke or biomass burning from forest in inner cities in China.

The compact Raman/elastic combined lidar performed almost continuous observations at Zhongshan, PRD, from Nov. 22 to Dec. 4, 2009. Figure 3(a) presented range-corrected signals from Nov. 27 to Dec. 3. Retrieval of the aerosol extinction profile was performed above 1 km, where the laser beam is fully within the telescopic field-of-view. Since the boundary layer is obviously different in two periods, from Nov. 27 to Nov. 29 and from Nov. 30 to Dec. 3, relative humidity and temperature on Nov. 27 and Dec. 3 are chosen as representative observing days in Fig. 3(b). The radiosonde data are from the Hysplit model. On both Nov. 27 and Dec. 3, the atmospheric condition was relatively dry since (relative humidity) RH was mostly lower than 60% up to 5.0 km. The slopes of the RH profile and the potential temperature (PT) profile on Nov. 27 showed a sudden change at the height of about 2.5 km, indicating the top of the (planetary boundary layer) PBL located between 2 and 3 km. A haze plume was also detected within the PBL from Nov. 27 to Nov. 28. And RCS was very high from 0.9 km uplifting the boundary layer and the haze layer. The PT profile also indicated a clear inversion at 2.5 km which coincides with the maximum RH values observed and thus indicates the arrival of air masses with different origin above and below the inversion in section 3.1.2. On Dec. 3, the vertical distribution of potential temperature suggested nearly stable in the 1–1.7-km altitude range. These facts supported the existence of relative homogeneous dry aerosol layer within the 1.7 km and PBL was approximately decreasing to 1.5 km.

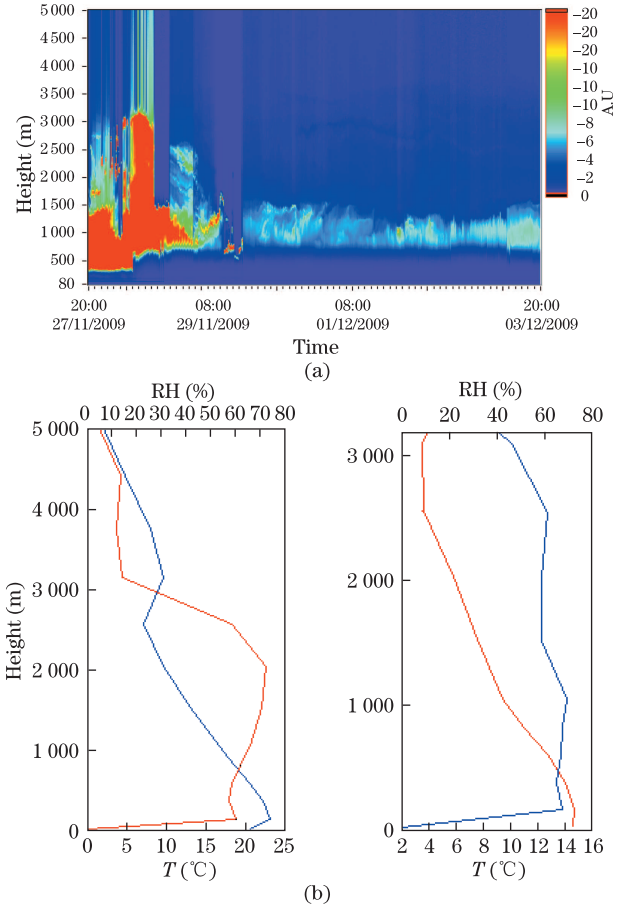

Fig. 3. (Color online) (a) RCS signal profiles from Nov. 27 to Dec. 3, 2009; (b) relative humidity (RH blue) and potential temperature (PT red) respectively on Nov. 27 and Dec. 3, 2009.

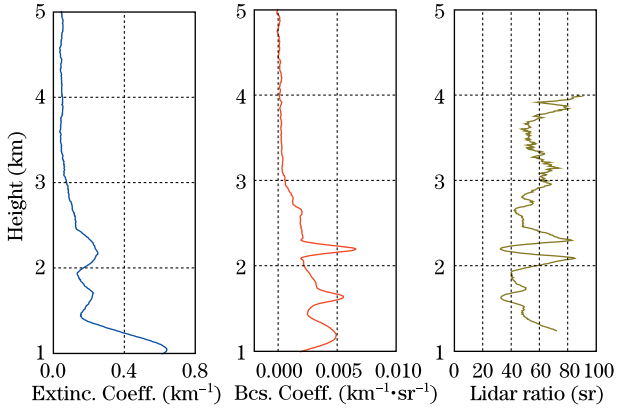

Fig. 4. Aerosol extinction coefficient, backscatter coefficient, and lidar ratio at 18:53-20:50 (LST), Nov. 27, 2009.

Extinction, backscatter, and lidar ratio profiles measured at night from 18:53 to 20:50 on Nov. 27 and from 19:30 to 21:30 on Dec. 3 are displayed in Figs. 4 and 5. The city reported up to five consecutive days of haze and dust at the end of Nov. (http://www.neworiental.org/publish/portal0/tab1127/info459530.htm). Figure 4 shows the optical properties of aerosols observed on Nov. 27 in the haze pollution episode. In this episode, the aerosol extinction profile reached a height of about 4 km, but most of the pollution aerosol was below 3 km. The aerosol extinction coefficient reached the maximum value of 0.65 km^{-1} at 1.2-km height. In this layer the lidar ratio profile is a bit variable with an average value of 47 sr. One more layer can also be distinguished from the extinction or backscatter profile with much larger and more variable lidar ratio at approximately 2.3 km. The higher mean lidar ratio value of 69±12 sr suggests aerosol content of a type different from that in the adjacent layers which implies different particle microphysical properties below and above 2 km. Then the backscatter coefficient in the 3–4 km layer was relatively constant in time, and the observed lidar ratio had an average value of 53 sr.

Figure 5 shows the optical properties of aerosols observed on Dec 3 in the moderate pollution episode. At the lay of the height from 2 to 3 km, the lidar ratio was variable with an average value of 58 sr. It also means the boundary layer is well mixed with stable aerosol sources. The lack of significant vertical variability of the lidar ratio suggests the presence of aerosol of the same source air masses.

Lidar ratio values are given up to 3–4 km, while Angstrom exponent values are also cut to 3.5 km. Angstrom exponent, which describes the wavelength dependence of the particle extinction coefficient is calculated as $A = -\{\ln[\alpha(\lambda_1)/\alpha(\lambda_2)]\}/[\ln(\lambda_1/\lambda_2)]$ and the wavelength pairs of 355/532 nm is used in this study. The Angstrom wavelength exponent ranged from 1.25 to 1.82, indicating the presentence of small particles. The corresponding total depolarization ration (DPR) was variable from 0.14 to 0.21, which suggests the sphere particles. According to optical properties of different aerosol types, the aerosol measured in our experiment may be constituted of the industrial aerosols and aerosols from the biomass burning. The lidar ratio, Angstrom exponent and DPR on Nov. 27, Nov. 28, Dec. 2, Dec. 3, Dec. 4 of the aerosol layer and are shown in Figs. 6 and 7.

The corresponding 4 day backward trajectories during the haze period (ending at Nov. 28) and moderate pollution (ending at Dec. 4) from Nov. 27 to Dec. 3 are shown in Fig. 8. In the haze period (Fig. 8(a)), the air mass below 0.5km is from the southeast coast China. The high lidar ratio and a low total depolarization ratio suggest the presence of light-absorbing spherical aerosol species such as soot. Soot is released from incomplete combustion of carbonaceous fuels, and it is frequently found in Shanghai during the heating period in winter. The great variability of lidar ratio also shows fine-mode aerosols mixed with sea salt and industrial aerosol. At the heights of 0.5 and 1.5 km, the lidar ratio of haze layer 47 sr is smaller than haze measurements from Cateese indicating larger particles in this experiment.

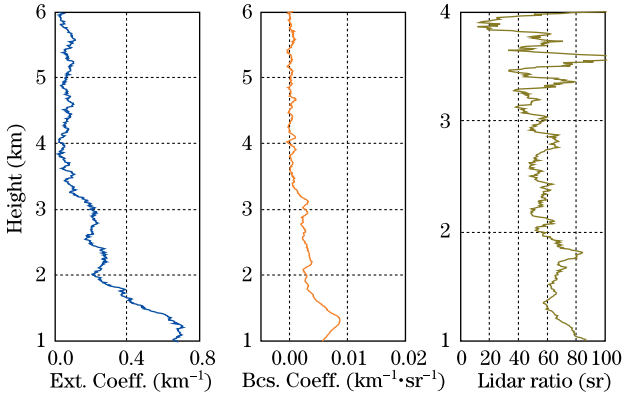

Fig. 5. Aerosol extinction coefficient, backscatter coefficient, and lidar ratio at 19:30-21:30 (LST), Dec. 3, 2009.

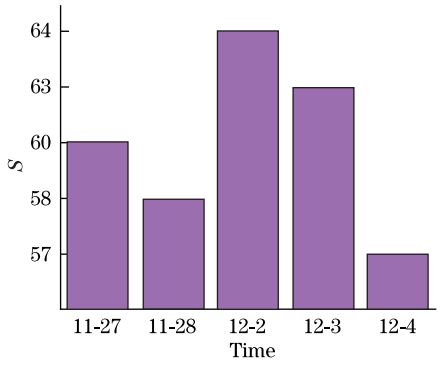

Fig. 6. Lidar radio averaged in the five-day observation.

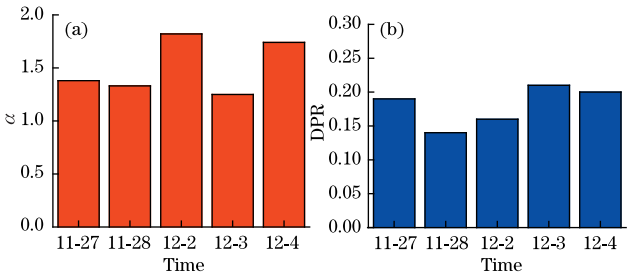

Fig. 7. (a) Angstrom exponent and (b) DPR during the observation day.

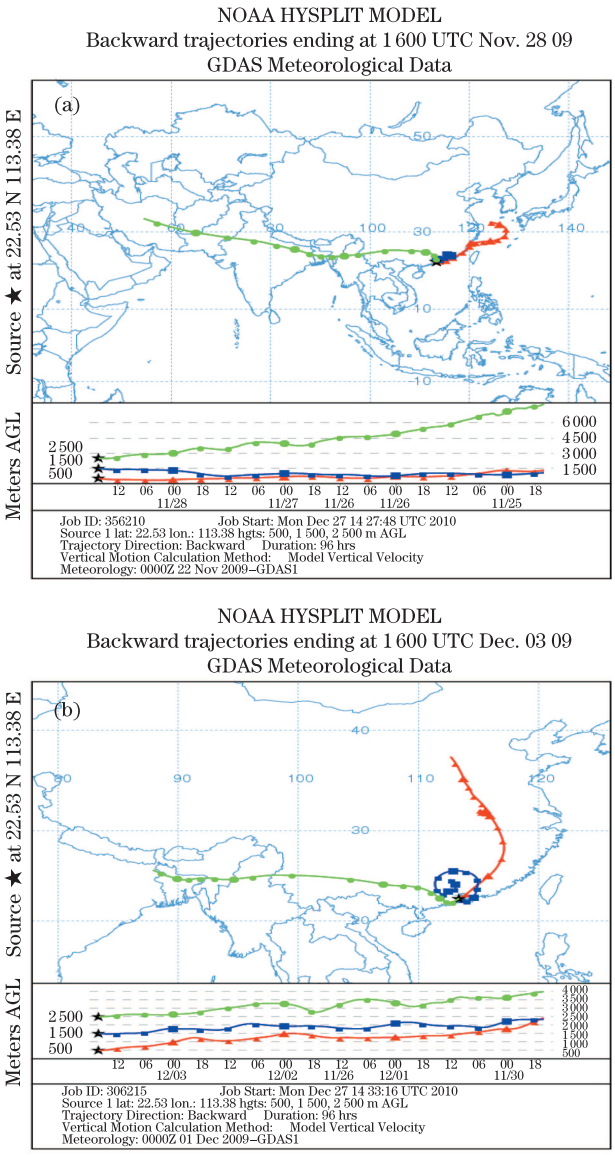

Fig. 8. Backward trajectories ending at Zhongshan, South China at 16:00 UTC on (a) Nov. 28, 2009 in haze pollution episode and (b) Dec. 3, 2009 in the moderate pollution episode.

In the moderate pollution period (Fig. 8(b)), the air mass below 0.5 km is different from the haze period. It came from the inner cities of China. The trajectories in the 0.5–1.5-km range show recirculation in the PRD region, collecting smoke from bios burning in this area, but probably also some fossil fuel pollution. The back trajectories above 2 km shown in Fig. 8(b) confirm the different lidar ratios that above 1.5-km air masses are transported from southern Asian. The air mass passed through northwest China. Usually, the region in northwest China is clean; however, from the fire spots based on level 2 Terra/ MODIS thermal anomalies/fire product (MOD14)[14] during the observing period, some fire is also detected in the Northwest. So the aerosol above 2 km maybe due to the combination of some pollution from the Tarim Basin in case of strong convection and the age smoke from the firing.

In conclusion, we conclude independent retrieval of both aerosol extinction and backscatter starting from Raman and elastic lidar signals. Heavily polluted situations usually occur at night. Particle extinction coefficients are as large as 600–800 Mm^{-1} in the middle and upper part of the haze at the end of Nov., 2009 PRD China. The Angstrom wavelength exponent indicates the presentence of small particles. The DPR value from 0.14 to 0.21 suggests the sphere particles. In the haze period, the great variability of lidar ratio shows fine-mode aerosols mixed with sea salt and industrial aerosol from southeast coast China. In the usual moderate pollution day, the aerosol measured in our experiment may be constituted of the industrial aerosols and aerosols from the biomass burning in inner cities.

References

1. D. Wu, X. Deng, X. Bi, F. Li, H. Tan, and G. Liao. Journal of Tropical Meteorology **13,** 77 (2006).
2. D. Wu, X. Tie, C. Li, Z. Ying, A. K. H. Lau, J. Huang, X. Deng, and X. Bi, Atmos. Environ. **39,** 6568 (2005).
3. C. Chan and X Yao, Atmos. Environ. **42,** 1 (2008).
4. A. Ansmann, U. Wandinger, M. Riebesell, C. Weitkamp, and W. Michaelis, Appl. Opt. **31,** 7113 (1992).
5. A. Ansmann, M. Riebesell, and C. Weitkamp, Opt. Lett. **15,** 746 (1990).
6. D. Müller and M. Tesche, Geo. Res. Lett. 33 L20811 2006.
7. J. Ackermann, J. Atmos. Oceanic Technol. **15,** 1043 (1998).
8. A. Ansmann and D. Muller, *Lidar Range-resolved Optical Remote Sensing of The Atmosphere* (Springer, Germany 2004) p112.
9. J. D. Klett, Appl. Opt. **24,** 1638 (1985).
10. F. G. Fernald, B. M. Herman, and J. A. Reagan, J. Appl. Meteorol. **11,** 482 (1972).
11. Y. Sasano and H. Nakane, Appl. Opt. **23,** 11 (1984).
12. O. Dubovik, B. N. Hollben, and T. F. Eck, J. Htmos. Sci. **59,** 590 2007.
13. R. R. Draxler and G. D. Rolph, "HYSPLIT (Hybrid Single-Particle Lagrangian Integrated Trajectory)," model access via NOAA ARL READY web site, http://www.arl.noaa.gov/ready/HYSPLIT4.html 2003.
14. Y. J. Kaufman, C. O. Justice, and C. P. Flynn, J. Geophys. Res. Atmos. **103,** 32215 (1998).